THE TUNGSTEN - P TYPE SILICON POINT CONTACT DIODE

Albert J. Kerecman
Semiconductor Devices & Integrated Electronics Technical Area
US Army Electronics Technology & Devices Laboratory (ECOM)
Fort Monmouth, New Jersey 07703

Abstract

Video detection at 90 GHz, 890 GHz, 28.3 THz, and 474 THz is examined with respect to whisker advancement. Reproducible behavior of I-V curves is obtained and correlated with the RF data. A significant thermal effect is shown to compete with conventional barrier rectification. Micrographic analysis coupled with microhardness measurements clearly demonstrates that the tungsten whisker exerts sufficient pressure to deform the silicon surface of the diodes.

Introduction

Point contact devices have played a major role in the detection, mixing, and harmonic generation of coherent sources from the microwave to the infrared.[1-8] Particular success has been obtained with tungsten - p type silicon[5] and the metal-oxide-metal devices.[9-12] The prime thrust of this effort is to characterize the behavior of the tungsten - p type silicon, run-in, point contact diode from the millimeter wave to the visible region.

Theory

There are two theoretical bases upon which to explain the detailed behavior of the barriers formed between metals and semiconductors. The first, the diffusion theory, assumes a barrier thickness large compared to the mean free path, so that the electron experiences numerous collisions within the barrier region. Mott[13] and Schottky[14] barriers are specific examples of the diffusion theory. The second model is the diode theory of Bethe.[15] Here, image force lowering of the barrier is taken to be a function of the applied voltage, electrons tunneling the barrier lower its effective height, and the work function of the surface is a variable over the contact area. The above models have had numerous modification[16-21] and only recently with the advent of the Schottky barrier devices has some semblance of order appeared.

Diode Description

The point contact devices used in this study consisted of a tungsten whisker 0.001 inch in diameter, electrolytically etched in NaOH solution to a fine point, in contact with a p type silicon wafer having a resistivity of 0.007 Ω cm. The silicon wafer is polished, etched in HF acid, and rinsed in distilled water. The diodes were housed in two commercially built mixer mounts (RG99/U), one commercially built multiplier (RG 98/U to RG 135/U), and a lab built open structure unit. This latter unit consisted of a differential micrometer for run-in of 5×10^{-6} inches resolution and a spherical reflector mounted on a translational stage with three degrees of freedom.

For reference, the equivalent circuit of the point contact diode is given in Fig. 1, where R_s is the spreading resistance, R_b is the barrier resistance, C_b is the barrier capacitance, and L_w is the whisker inductance. In this equivalent circuit, R_b and C_b are variable and functionally dependent on applied voltage.

$$I = I_o \left(e^{qv/kT} - 1\right) \quad (1)$$

$$R_b = kT/qI \quad (2)$$

$$C_b = (\phi_o - V)^{-1/2} \quad (3)$$

while L_w and R_s are independent of applied voltage but are dependent upon mechanical configuration and contact pressure.[22] The spreading resistance is dependent upon the bulk resistivity of the semiconductor and is inversely proportional to the radius of the point contact.[23] The barrier capacitance depends directly upon the area of the contact and inversely upon the thickness of the barrier. This capacitance shunts the non-linear resistance, R_b, of the barrier, becoming a more effective by-pass as frequency increases.[24]

Diode Characterization

Initial efforts to obtain reproducible behavior of the diode characteristics only resulted in general observations due to the coarseness of the differential screws used in the commercial units and to the method of initial contact observation.

The use of a Lansing 22 505 differential micrometer is an open structure gave an order of magnitude improvement in whisker advancement resolution over the commercial units. A method of initial contact observation was devised as follows:

(1) Surface cleaning of silicon wafer with "Bioden," acetylcellulose replicating film (used by electron microscopists).

(2) Visual determination of initial contact by impinging HeNe laser through the point contact area to the spherical reflector and observing the magnified back projection.

(3) Initial electrical contact dermined with a Tektronix 1A7A.

A successful initial contact will occur when the noise signal, observed on an oscilloscope (step 3), changes its character prior to any whisker bending (step 2). Other criteria lead to anomalous results.

I-V Characteristics

Given a proper initial contact, a characteristic curve sequence as shown in Fig. 2 is observed. It is the one sequence occurring repeatedly in initial contact and run-in on all samples tested. The initial contact corresponds to the outermost curve of picture 1. As pressure is increased, or better, as advancement of the whisker is continued, the curves, forward and back, display an increase in differential conductance ($g = dI/dV$) until a maximum is reached (innermost curve of pictures 2 and 3). Further whisker advancement then causes a decrease in the differential conductance to values less than those produced by the initial contact (pictures 3 and 4).

The characteristic curves of Fig. 2 were found to be completely reproducible from experiment to experiment. Changes induced during the time of whisker advancement are reversible and the entire process cyclical providing that the elastic limit of the whisker is not exceeded.

If the diode is set to the condition depicted by the outermost curve of picture 4, Fig. 2, and a 1 mA current limited pulse of approximately 50 V is applied to the diode in the forward direction, the I-V characteristic is radically changed as shown in the outer curve of picture 5. Now, with further whisker advancement the differential conductivity once again increases, but no longer exhibits a reversal as noted in pictures 3 and 4. One does note, however, an improvement in rectification efficiency (front to back resistance ratio). The sequence of Fig. 2, therefore, shows the behavior of a typical point contact diode made by the run-in process and the difference between a point contact and a welded contact characteristic.

Interpretation of the DC Characteristics

In an attempt to obtain correlation between theory and the experimental observations of diode behavior as a function of whisker pressure, it was postulated that a mechanical deformation of both the silicon surface and tungsten whisker occurred. To establish credibility for the following arguments, a detailed micrographic study was carried out. Electron microscopy replicating techniques were employed here to observe the surface of the diode,[25] (Fig. 3). Here, since the shadowcast angle was 45°, the length of the shadow is equal to the height of the hillock in the replica which is equal to the depth of the valley in the silicon surface. In particular, the depth is 1300 Å and, in this case, is equal to the diameter.

Figure 4 is an electron micrograph of a typical tungsten whisker; the dark area is whisker and the gray periphery is contamination produced in the electron microscope. The magnification is identical to that of the previous micrographs showing the correlation of whisker and valley size.

Now, by establishing the hardness values for silicon and tungsten, it will be shown that the tungsten whisker is, in fact, capable of penetrating the surface of the silicon wafer. In the past, the assumption has been that silicon was much harder than the tungsten whisker and, therefore, no penetration was possible. This assumption is not correct for heavily drawn tungsten wire.[26]

The hardness of silicon is well documented,[27] however, the hardness of tungsten is dependent upon the number of dislocations, and as the wire is drawn, the dislocation count increases. A specific study was performed on the tungsten wire (0.001")$_0$ and the silicon wafer used in the present experiments.[28] The measured value of the silicon is $KHN_{50} = 980\ Kg/mm^2$ (Fig. 5 a) and that for the tungsten is $KHN_{50} = 1020\ Kg/mm^2$ (Fig. 5b). Since the tungsten is at least as hard as the silicon and the geometry of the two surfaces greatly favors the whisker, it seems conclusive that the tungsten whisker does penetrate the silicon surface upon making contact.

Coordinated studies, using the visual aid technique concomitant with the curve tracer, indicate that a maximum in the differential conductivity occurs approximately when maximum pressure is transmitted from the whisker to the wafer. As whisker advancement is further increased, the whisker bends and is no longer capable of sustaining the force it did prior to bending, since shearing deformation now becomes a significant factor.

We now look at the spreading resistance to account for the behavior of the characteristic curves. When a contact is first initiated, the contact area can be approximated by a circular plane area of very small dimensions. Here, the resistance is simply that of parallel plates separated by the resistive layer and

$$R = \rho l/a \tag{4}$$

or in the case of a circular contact

$$R = \rho l/\pi r^2 \tag{5}$$

When the whisker is advanced, the planar model gives way to a spherical contact of radius r, due to deformation of the silicon surface. Here, the contacting surface area prior to whisker bending is simply that of a hemisphere, $2\pi r^2$. The total resistance encountered is then given by,[29]

$$R_s = (\rho/2\pi) \int_{r_o}^{\infty} r^{-2} dr = \rho/2\pi r_o \tag{6}$$

where r_o is the radius of the whisker tip. Now, the whisker advances no further into the semiconductor and as the run-in proceeds, the whisker begins to bend causing a rotation of the hemispherical tip. First, as this rotation occurs, caused by the whisker bending, the surface area of the contact between whisker and wafer is reduced, since one side of the hemisphere rolls or presses into the semiconductor and the other side departs from the semiconductor surface by an equal amount. Now, the contact is no longer hemispherical, but, at best, is approximately the surface of one quarter of a sphere. This new surface is now better approximated by the initial condition of a planar surface, than that of a spherical surface. Therefore, due to the fact that the planar surface, for equal contact areas, produces a greater spreading resistance than the hemispherical surface, by a factor of $1/r_o$, a maximum in the conductivity followed by a subsequent decrease is evident.

Furthermore, it is well established that the band gap in silicon decreases with increasing pressure and temperature.[30,31] This, in light of the previous argument on whisker bending, would also point to a maximum in the conductivity, occurring when the greatest pressure is applied to the semiconductor. A similar argument can be made for barrier capacitance, showing a minimum in the capacitance at initial contact followed by an increase as the whisker indents the semiconductor, and then by a decrease as the bending causes the surface area of contact to decrease.

Picture 5, Fig. 2 shows curves which are no longer representative of a point contact diode. Here, the high voltage spike was sufficient to cause sputtering, resulting in either a Schottky barrier or an alloyed junction. In this case, no maximum in the conductivity occurred, rather, advancement of the whisker produced an increase in conductance up to some maximum value. No reversal was evident, indicating that a fixed area contact had been established and that no increase in R_s was now possible as whisker being occurred.

Responsivity Vs. Frequency Measurements & Interpretation

Essentially, identical experiments on detector responsivity were conducted at 94 GHz, 890 GHz, 28.3 THz, and 474 THz. The devices were used as voltage detectors working into a 1 MΩ load. Figure 6 shows a composite of the experimental data. Responsivity versus whisker advancement data at 94 and 890 GHz exhibits a peak-valley-peak characteristic which corresponds to and correlates with the point contact I-V run-in sequence of Fig. 2. At 28.3 and 474 THz the polarity of the detector voltage reverses and the responsivity as a

function of whisker advancement is essentially constant with a slight decrease observed at the initial contact.

The data can be understood by assuming a point contact diode model which includes thermoelectric and photoelectric generators as shown in Fig. 7. From this model, one should expect a responsivity curve versus frequency similar to that of Fig. 8 to result.

Conclusions

The present study has clarified the behavior of diodes, comprised of pointed tungsten whiskers in pressure contact with heavily doped p type silicon, as a function of frequency. The DC characteristics have been correlated with RF performance at four major frequencies: 90 GHz, 890 GHz, 28.3 THz, and 474 THz.

The existence of a significant thermal effect has been identified and shown to compete with conventional barrier rectification. At the lower frequencies, barrier rectification dominates and as the frequency is increased, the thermoelectric effect tends to become more dominant as the rectification efficiency degrades due to the shunting action of the barrier capacitance.

Finally, through micrographic analysis it has been shown that the tungsten whisker exerts sufficient pressure to measurably deform the silicon surface. This is believed to be the first clear demonstration that such deformations actually occur. Previously, it had been supposed that the tungsten whisker point would consistently yield before the silicon surface.

Acknowledgments

The author is deeply indebted to his thesis advisor, Dr. F. A. Brand, for his time and effort unselfishly donated, to G. F. Wilson for the designs and fabrication of support equipment, to C. F. Cook, Jr. and A. Dunlap for the micrographic studies, and to W. F. Nye for the hardness measurements. Special thanks are due to J. G. Small for instilling patience and to R. Winton for much help with the RF data.

References

1. M.I.T. Radiation Laboratory Series, L. N. Ridenour, ed., McGraw Hill.

2. W. M. Sharpless, Bell System Tech. J., Vol. 35, pp. 1385-1402, November 1956.

3. W. M. Sharpless, Bell System Tech. J., Vol. 42, pp. 2496-2499, September 1963.

4. C. A. Burrus, Jr., Proc. IEEE, Vol. 54, pp. 575-587, April 1966.

5. R. J. Bauer, M. Cohn, J. M. Cotton, Jr., and R. F. Packard, Proc. IEEE, Vol. 54, pp. 595-605, April 1966.

6. L. O. Hocker, A. Javan, and D. Ramachandra Rao, Appl. Phys. Ltrs., Vol. 10, No. 5, pp. 147-149, 1 Mar 67.

7. V. Daneu, D. Sokoloff, A. Sanchez, and A. Javan, Appl. Phys. Ltrs., Vol. 15, No. 12, 15 Dec 69.

8. K. M. Evenson, J. S. Wells, and L. M. Matarrese, Appl. Phys. Ltrs., Vol. 16, No. 6, 15 Mar 70.

9. L. O. Hocker, A. Javan, and D. Ramachandra Rao, "Absolute Frequency Measurement and Spectroscopy of Gas Laser Transitions in the Far Infrared," Appl. Phys. Ltrs., Vol. 10, p. 147, 1 Mar 67.

10. L. O. Hocker, et al, Appl. Phys. Ltrs., Vol. 12, No. 12, pp. 401-402, 15 Jun 68.

11. S. I. Green, P. D. Coleman, and J. R. Baird, Polytechnic Institute of Brooklyn, Symposium on Submillimeter Waves, 1 Apr 70.

12. L. M. Matarrese and K. M. Evenson, Appl. Phys. Ltrs., Vol. 17, No. 1, pp. 8-10, 1 Jul 70.

13. N. F. Mott, "The Contact Between a Metal and an Insulator or Semiconductor," Proc. Cambridge Phil. Soc., Vol. 34, p. 568. (See also Proc. Roy. Soc., A171, 27)

14. W. Schottky, "Semiconductor Theory of the Barrier Film," Naturwissenschaften, Vol. 26, 843; also, "Simplified and Extended Theory of Barrier-Layer Rectifiers," Z. Physik 118, pp. 539-592; also, W. Schottky and E. Spenke, Wiss. Veroff. Siemenswerke, Vol. 18, p. 225.

15. H. A. Bethe, "Theory of the Boundary Layer of Crystal Rectifiers," M. I. T. Radiation Lab Report, 43-12, November 1942.

16. E. O. Kane, "Theory of Tunneling," J. Appl. Phys., Vol. 32, p. 83, January 1961.

17. F. A Padovani and R. Stratton, "Experimental Energy-Momentum Relationship Determination Using Schottky Barriers," Phys. Rev. Ltrs., Vol. 16, p. 1202 (1966).

18. F. A Padovani and R. Stratton, "Field and Thermionic-Field Emission in Schottky Barriers," Solid State Elct., Vol. 9, p. 965 (1966).

19. J. W. Conley and G. D. Mahan, "Tunneling Spectroscopy in GaAs," Phys. Rev., Vol. 161, p. 681 (1967).

20. C. R. Crowell and S. M. Sze, "Current Transport in Metal-Semiconductor Barriers," Solid State Elct., Vol. 9, p. 1035 (1966).

21. V. L. Rideout and C. R. Crowell, "Effects of Image Force and Tunneling on Current Transport in Metal - Semiconductor (Schottky Barrier) Contacts," Solid State Elct., Vol. 13, p. 993 (1970).

22. D. A. Fleri and L.D. Cohen, IEEE Trans., MTT-21, No. 1, pp. 39-43, January 1973.

23. Torrey and Whitmer, "Crystal Rectifiers," Rad. Lab. Series, Vol. 15, pp. 82-85, McGraw-Hill (1948).

24. Torrey and Whitmer, loc. cit., Vol. 19, pp. 24, 70-77, 97.

25. Private study for the author by C. F. Cook, Jr. and A. Dunlap (USAECOM, Fort Monmouth, N.J.), January 1971.

26. Tabor, The Hardness of Metals, p. 171, Oxford at the Clarendon Press (1951).

27. H. O'Neill, Hardness Measurements of Metals and Alloys, p. 168 and 192, Chapman and Hall (1967).

28. Private study for the author by W. F. Nye (USAECOM, Fort Monmouth, N.J.), January 1971.

29. Henisch, Rectifying Semi-Conductor Contacts, pp. 218-220, Oxford at the Clarendon Press (1957).

30. W. Paul, "The Effect of Pressure on the Properties of Germanium and Silicon," J. Phys. Chem. Solids, Vol. 8, p. 196 (1959).

31. Hrostowski, Semiconductors, p. 451, N.B. Hannay, ed., Reinhold (1959).

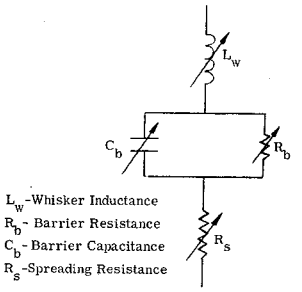

Fig.1 Point contact diode equivalent circuit.

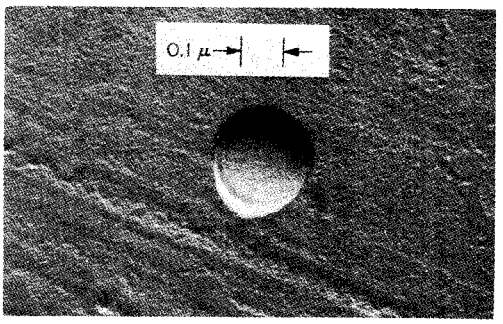

Fig.3 Electron micrograph of silicon surface.

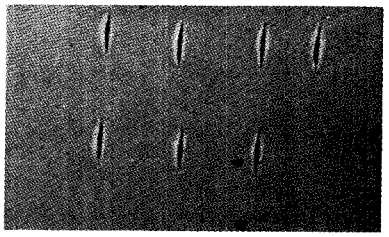

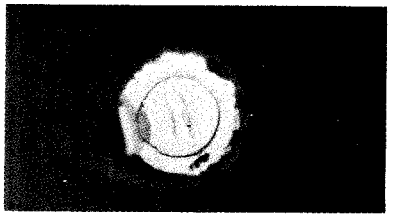

Fig.5 a. Knoop hardness indents in silicon wafer.
b. " " " " tungsten whisker.

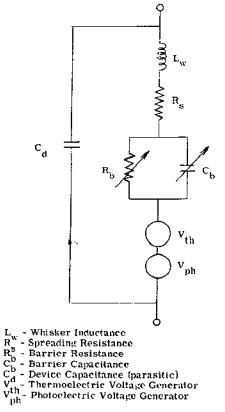

Fig.7 Proposed diode equivalent circuit.

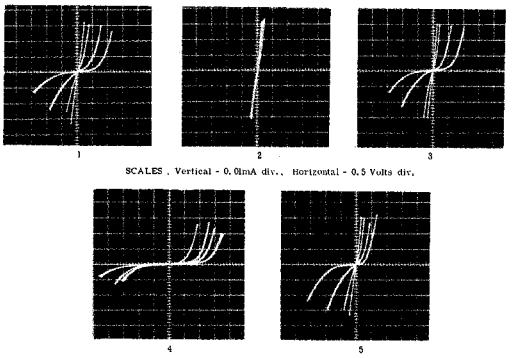

Fig.2 Diode run-in, I-V sequence.

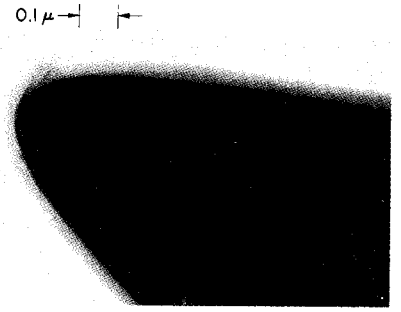

Fig.4 Electron micrograph of tungsten whisker.

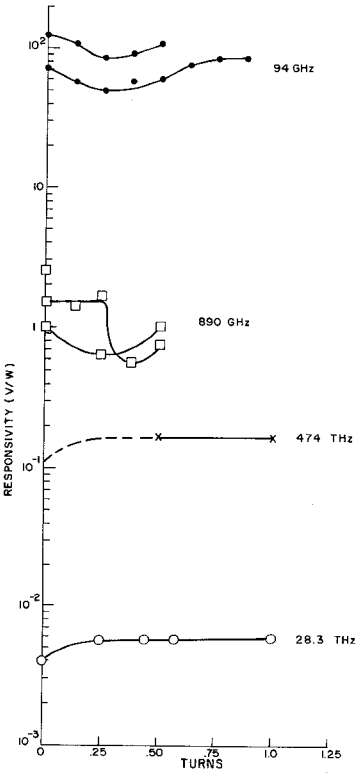

Fig.6 Diode responsivity versus whisker run-in.

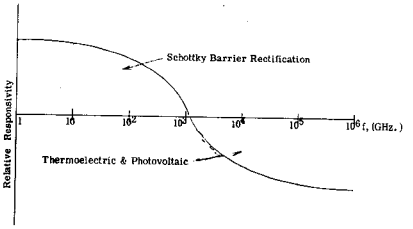

Fig.8 Relative responsivity versus frequency.